Available online at www.sciencedirect.com
SCIENCE DIRECT®
ELSEVIER
International Journal of Heat and Mass Transfer 48 (2005) 3880–3888
International Journal of HEAT and MASS TRANSFER
www.elsevier.com/locate/ijhmt

Technical Note

A new approach for thermal performance calculation of cross-flow heat exchangers

Hélio Aparecido Navarro [a,*], Luben Cabezas-Gómez [b]

[a] *Departamento de Estatística, Matemática Aplicada e Computação, Instituto de Geociências e Ciências Exatas, Universidade Estadual Paulista "Júlio de Mesquita Filho", Av. 24-A, 1515, Cx. P178, CEP 13506-700, Rio Claro, SP, Brazil*
[b] *Departamento de Engenharia Mecânica, Escola de Engenharia de São Carlos, Universidade de São Paulo, Av. Trabalhador São-carlense, 400—Centro, CEP 13566-590, São Carlos, SP, Brazil*

Received 28 September 2004; received in revised form 3 March 2005

Abstract

A new numerical methodology for thermal performance calculation in cross-flow heat exchangers is developed. Effectiveness–number of transfer units (ε–NTU) data for several standard and complex flow arrangements are obtained using this methodology. The results are validated through comparison with analytical solutions for one-pass cross-flow heat exchangers with one to four rows and with approximate series solution for an unmixed–unmixed heat exchanger, obtaining in all cases very small errors. New effectiveness data for some complex configurations are provided.

Keywords: Thermal effectiveness; NTU; Cross-flow heat exchangers; Numerical simulation

1. Introduction

Due to wide range of design possibilities, simple manufacturing, less maintenance and low cost cross-flow heat exchangers are extensively used in industries e.g. petroleum, petrochemical, air conditioning, food storage, and others. Such heat exchangers are especially well suited for gas cooling and heating. The extensive use of these apparatus has generated the need for calculation method that accurately predicts their performance [1].

A comprehensive review of solution methods for determining effectiveness (ε or P)–number of transfer units (NTU) relationships for two-fluid heat exchangers with simple and complex flow arrangements is presented by Sekulic et al. [2]. The methods were categorized by the authors as: analytical methods for obtaining exact solutions, approximate methods, curve-fit to the results from the exact solutions, numerical methods, matrix formalism, and methods based on exchanger configuration properties, as the use of flow reversal symmetry of exchanger configurations. In conformity to the authors continuing efforts to design more efficient systems, more compact exchangers, or specific operating conditions may require effectiveness–NTU formulae for a new heat exchanger, not reported in the literature. Using some of these methods Pignotti and Shah [3] obtained 18 effectiveness–NTU explicit formulas for new arrangements.

The main aim of this article is to provide a new numerical methodology for thermal performance

* Corresponding author. Fax: +55 19 3534 8250.
E-mail addresses: helio@rc.unesp.br (H.A. Navarro), lubencg@sc.usp.br (L. Cabezas-Gómez).

0017-9310/$ - see front matter
doi:10.1016/j.ijheatmasstransfer.2005.03.027

Nomenclature

A	exchanger outer total heat transfer area, m^2
A_{fr}	exchanger total frontal area, m^2
C	heat capacity rate, W/K
C^*	heat capacity rate ratio, C_{min}/C_{max}, dimensionless
L	total heat exchanger flow length, m
N_c	number of circuits
N_e	number of elements per tube
N_r	number of rows in the heat exchanger
N_t	number of tubes per row
NTU	number of transfer units, UA/C_{min}, dimensionless
P	temperature effectiveness, $(T_{c,o} - T_{c,i})/(T_{h,i} - T_{c,i})$, dimensionless
q	heat transfer rate, W
R	temperature ratio, $(T_{h,i} - T_{h,o})/(T_{c,o} - T_{c,i})$, dimensionless
T	temperature, K
U	overall heat transfer coefficient, W/m^2K

Greek symbols

δ	denotes difference
Δ	denotes difference
ε	conventional heat exchanger effectiveness, q/q_{max}, dimensionless
Γ	dimensionless parameter defined by Eqs. (7) and (12)

Subscripts

c	cold fluid side of heat exchanger
h	hot fluid side of heat exchanger
i	inlet conditions
max	maximum value
min	minimum value
o	outlet conditions

Superscript

e	element

calculation of cross-flow heat exchangers. The proposed methodology is based on physical concepts and it is characterized by the division of the heat exchanger in a number of small and simple one-pass mixed–unmixed cross-flow heat exchangers. The present approach allows obtaining effectiveness data for new configurations.

At present, solutions can be getting only for configurations where the external fluid is unmixed (considered here as air flowing over finned tube bundles) and the tube fluid is well mixed in each tube cross-section and unmixed between passes. Then, heat exchangers with one to several tubes can be analyzed, including different tube fluid circuiting configurations.

Next, in Section 2, it is presented the proposed numerical methodology for thermal performance parameters calculation. In Section 3 simulation results are presented and compared with available solutions from literature, considering cross-flow heat exchangers with simple and complex flow arrangements. Finally, the conclusions of the paper are presented in Section 4.

2. Methodology development

2.1. Governing equations for one-pass cross-flow heat exchanger

The governing equations presented in this section are those developed for a cross-flow heat exchangers with one fluid mixed and another unmixed following [4]. These are the basic equations applied in the proposed numerical solution methodology. Fig. 1 shows the

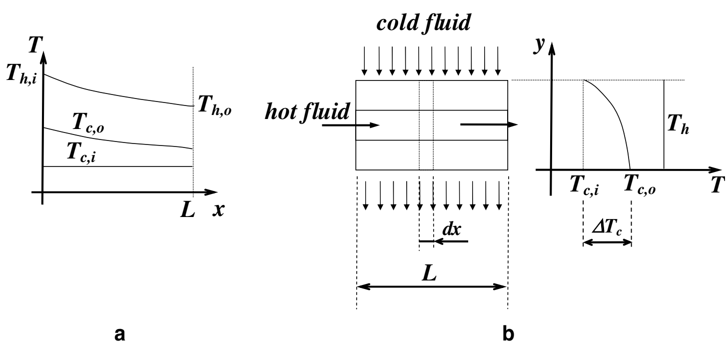

Fig. 1. (a) Air and fluid temperature variations in the longitudinal direction with respect to the fluid flow and (b) cross-flow air temperature variation in a differential volume element of the heat exchanger.

temperature conditions for one-pass cross-flow mixed–unmixed heat exchanger having one row. It is considered that tube side fluid is perfectly mixed in the tube cross-section and external fluid is perfectly unmixed, i.e., there are fins in the airside. It is also assumed for convenience that the mixed fluid is hot and the unmixed is cold. The equations are also valid when the unmixed fluid is hot and the mixed is cold. For this condition the subscripts hot and cold must be interchanged.

Fig. 1(a) illustrates the hot and cold temperature variations along a tube of length L whereas Fig. 1(b) shows both temperature variations along the cold fluid flow length in the differential length ($\mathrm{d}x$). In this infinitesimal section, the cold mass flow rate is small and therefore the hot fluid temperature is constant. An energy balance in the differential length, $\mathrm{d}x$, for the hot and cold fluids can be written as

$$\delta q = -C_\mathrm{h} \cdot \mathrm{d}T_\mathrm{h} \tag{1}$$

$$\delta q = \mathrm{d}C_\mathrm{c} \cdot \Delta T_\mathrm{c} \tag{2}$$

where $\Delta T_\mathrm{c} = (T_\mathrm{c,o} - T_\mathrm{c,i})$ is the mean temperature variation of the cold fluid in the differential length, $\mathrm{d}x$. Using the fact that in the differential section $\mathrm{d}x$, the cold mass flow rate is small in comparison with the hot mass flow rate, must be assumed that the hot capacity rate, C_h, is constant in the section and a differential heat capacity rate ratio must be expressed as

$$\mathrm{d}C^* = \frac{\mathrm{d}C_\mathrm{c}}{C_\mathrm{h}} \to 0 \tag{3}$$

Considering Eq. (3) and the temperature conditions (Fig. 1), a condenser type of effectiveness expression is applicable. Then, using the effectiveness definition, a parameter Γ that expresses the 'local effectiveness' in the differential length $\mathrm{d}x$ can be written as [4]

$$\Gamma = \frac{\Delta T_\mathrm{c}}{(T_\mathrm{h} - T_\mathrm{c,i})} = 1 - \mathrm{e}^{-\frac{U\mathrm{d}A}{\mathrm{d}C_\mathrm{c}}} \tag{4}$$

Assuming that both the cold flow and heat transfer area A distributions are uniform, the following relations are valid

$$\frac{\mathrm{d}C_\mathrm{c}}{\mathrm{d}A_\mathrm{fr}} = \frac{C_\mathrm{c}}{A_\mathrm{fr}} = \mathrm{const} \tag{5}$$

$$\frac{\mathrm{d}C_\mathrm{c}}{\mathrm{d}A} = \frac{C_\mathrm{c}}{A} \tag{6}$$

Thus, along the tube length L

$$\Gamma = 1 - \mathrm{e}^{-\frac{UA}{C_\mathrm{c}}} = \mathrm{const} \tag{7}$$

Combination of Eqs. (1), (2) and (4) and separation of variables lead to

$$\frac{\mathrm{d}T_\mathrm{h}}{T_\mathrm{h} - T_\mathrm{c,i}} = -\Gamma \mathrm{d}C^* = -\Gamma \frac{C_\mathrm{c}}{C_\mathrm{h}} \frac{\mathrm{d}A_\mathrm{fr}}{A_\mathrm{fr}} \tag{8}$$

In Eq. (8) it should be noted that C_c, C_h and A_fr are the total magnitudes and are not variables. As mentioned, the developed governing equations are valid for one-pass cross-flow heat exchanger, one fluid mixed and another unmixed. For this kind of heat exchanger, the integration of Eq. (8) can easily be done analytically obtaining the ε–NTU relations (see Eq. (15) latter). Nevertheless, cross-flow heat exchangers for engineering applications, commonly, have a complex flow arrangement with several circuits and rows. For these exchangers the solution of this system of equations (Eqs. (1)–(8)) is not trivial. In these cases the performance of derivation and integration founded in Eq. (8) is difficult due to two reasons: due to a non-validity of Eqs. (6) and (7) for the overall heat exchanger area, and due to a variation of temperature distribution of the cold (unmixed) fluid, $T_\mathrm{c,i}$, in each row of the heat exchanger. This leads to an application of numerical procedure to obtain a desired solution.

2.2. Numerical solution methodology

The proposed methodology is based on application of Eqs. (1)–(8) and consists in the following mean steps:

First step: The heat exchanger is divided into a set of three dimensional control volumes called elements identified by the triplet (i, j, k). The indices $1 \leqslant i \leqslant N_\mathrm{e}$; $1 \leqslant j \leqslant N_\mathrm{t}$; and $1 \leqslant k \leqslant N_\mathrm{r}$ represent the element position along a particular tube, the tube in each row, and the row, respectively. It should be noted that each element is modeled as a mixed–unmixed heat exchanger schematized in Fig. 2.

Second step: The system of governing equations of Section 2.1 are integrated and applied in each element separately. This leads to a system of algebraic equations for each element and consequently for a whole heat exchanger.

Third step: The above system of equations for a whole heat exchanger is solved iteratively. It is done following tube fluid circuits along the heat transfer surface through indices i, j, k management.

As the mathematical model employed (see Section 2.1) is valid for a one-pass mixed–unmixed cross-flow

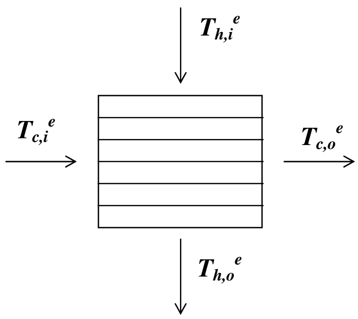

Fig. 2. Scheme of a mixed–unmixed heat exchanger.

heat exchanger, the size of all elements must be sufficiently small to ensure this condition. This means that should be used a large enough number of elements. Therefore, each element work as an independently heat exchanger connected to others by the tube fluid circuits. Solving iteratively the integrated algebraic equations in each of these small heat exchangers (i.e., elements) it is obtained the temperature distribution in the whole heat exchanger. The thermal performance parameters are founded through application of its definitions.

2.3. Algebraic equation system for an element

The algebraic equations for each element are obtained through the integration of the equations from Section 2.1. Firstly due to the small element size and validity of Eq. (3), it is assume that the hot fluid (mixed) temperature has a linear variation along a control volume, whereas the cold (unmixed) has an exponential variation. This way, the hot average element fluid temperature is expressed as

$$T_{\mathrm{h}}^{e} = 0.5\left(T_{\mathrm{h,i}}^{e} + T_{\mathrm{h,o}}^{e}\right) \tag{9}$$

where the superscript e is associated with a specific element (i, j, k). Now integration of Eq. (1) in the element leads to

$$q^{e} = -C_{\mathrm{h}}^{e}\left(T_{\mathrm{h,o}}^{e} - T_{\mathrm{h,i}}^{e}\right) \tag{10}$$

In obtaining the heat balance for the cold fluid, thought the integration of Eq. (2), and using Eq. (5), the following expression can be written

$$q^{e} = \Delta T_{\mathrm{c}}^{e}\int_{e} \mathrm{d}C_{\mathrm{c}} = \Delta T_{\mathrm{c}}^{e}\int_{e}\frac{C_{\mathrm{c}}}{A_{\mathrm{fr}}}\mathrm{d}A_{\mathrm{fr}} = \Delta T_{\mathrm{c}}^{e}C_{\mathrm{c}}^{e} \tag{11}$$

where C_{c} and A_{fr} are the total magnitudes and are not variables and $\Delta T_{\mathrm{c}}^{e} = T_{\mathrm{c,o}}^{e} - T_{\mathrm{c,i}}^{e}$ represents the mean cold fluid temperature difference in the element. To close the algebraic equation system integration of Eq. (4) in the element results in

$$\Gamma^{e} = \frac{\Delta T_{\mathrm{c}}^{e}}{\left(T_{\mathrm{h}}^{e} - T_{\mathrm{c,i}}^{e}\right)} = 1 - \mathrm{e}^{-\frac{(UA)^{e}}{C_{\mathrm{c}}^{e}}} \tag{12}$$

The last term of Eq. (12) is equal to that of Eq. (7). This is obtained because it is assumed that each element is equal to a one-pass mixed/unmixed cross-flow heat exchanger. Therefore, the equations of Section 2.1 are valid.

The relations (9)–(12) represent a closed system of equations to be solved for each element for five unknowns. There are five equations for five unknowns, namely: q^{e}, Γ^{e}, T_{h}^{e}, $T_{\mathrm{h,o}}^{e}$ and $\Delta T_{\mathrm{c}}^{e}$, knowing $T_{\mathrm{h,i}}^{e}$, $T_{\mathrm{c,i}}^{e}$, $(UA)^{e}$, C_{c}^{e} and C_{h}^{e}. To solve these equations for the whole heat exchanger, i.e. for all the elements interconnected, is needed an iterative procedure (see Section 2.4). The above system of five equations must be rearranging to obtain the following two equations for temperature calculation in each element:

$$T_{\mathrm{c,o}}^{e} = \frac{A + 2(1 - \Gamma^{e})}{2 + A}T_{\mathrm{c,i}}^{e} + \frac{2\Gamma^{e}}{2 + A}T_{\mathrm{h,i}}^{e} \tag{13}$$

$$T_{\mathrm{h,o}}^{e} = \frac{2 - A}{2 + A}T_{\mathrm{h,i}}^{e} + \frac{2A}{2 + A}T_{\mathrm{c,i}}^{e} \tag{14}$$

where $A = C_{\mathrm{c}}^{e}\Gamma^{e}/C_{\mathrm{h}}^{e}$. Eqs. (13) and (14) are used in the procedure described below.

During derivation of the governing equations (Section 2.1) and its discretization (present section) the following hypothesis were assumed in agreement with literature work [5]. The heat exchanger operates under steady state conditions. The heat losses to the surroundings are negligible (i.e. the heat exchanger is adiabatic). There are no thermal energy sources and sinks in the heat exchanger walls or fluids. The tube fluid is perfectly mixed in each cross-sectional area varying linearly through each element; and the external fluid (unmixed) is uniformly distributed at the inlet and outlet in each element, being their temperatures mean values in these regions. There are no phase changes in the fluid streams. The physical properties and heat transfer coefficients are constant for the heat exchanger surface. Considering these hypotheses, it is proposed a methodology that allows determining theoretical efficiency data. However, these data are very useful for heat exchanger design and rating procedures (e.g., [6]).

2.4. Procedure for thermal parameters calculation of heat exchanger

The effectiveness is calculated by the following procedure. Firstly are read the geometric data for a specific heat exchanger from a database. Then are defined the values of NTU, C^* and $C_{\min} = (C_{\mathrm{c}}$ or $C_{\mathrm{h}})$. For simulation purposes the $T_{\mathrm{c,i}}$, $T_{\mathrm{h,i}}$ and UA values are arbitrarily chosen, since ε depends only on NTU, C^*, and flow arrangement. Now the parameter Γ^{e} for each element is computed according to Eq. (12), where $(UA)^{e}$ is calculated using the number of elements and C_{c}^{e} and C_{h}^{e} are computed considering the mass flow corresponding to each element. As the developed procedure is valid only when the element unmixed fluid heat capacity is minimum, i.e. $C_{\mathrm{unmixed}}^{e}/C_{\mathrm{mixed}}^{e} \leqslant 1$ (see Section 2.1); the number of elements, N_{e}, should be chosen to ensure this condition.

The heat exchanger temperature distribution is calculated iteratively following the tube fluid circuiting using Eqs. (13) and (14). It should be noted that it is computed the temperature distribution for constant thermodynamics properties and mean overall heat transfer coefficient. For this reason the parameter Γ^{e} is constant for all elements. However, if it is considered the computation of the real temperature distribution, the parameters Γ^{e} as well as $(UA)^e, C_h^e$ and C_c^e should be computed for each element, using local properties and heat transfer coefficients. For both cases, the outlet cold and hot temperatures in each element are estimated using Eqs. (13) and (14). The convergence criteria is related to the mean cold fluid outlet temperature ($T_{c,o}$) and is also checked by the heat transferred rate q equality. Finally the effectiveness ε is computed by definition.

3. Results

In this section are discussed results obtained with the developed methodology. Firstly, simulation data are presented for one-pass cross-flow exchangers with n rows. These results are compared with the available analytical relations showing a very good agreement. Next, more complex heat exchanger configurations are tested through comparison with literature proposed solutions obtaining a very good agreement. Finally, for these configurations new effectiveness data are provided. To identify the heat exchanger geometries analyzed in this paper it is used the notation $G_{N_p,N_{rp}}$ from [6]. The two subscripts represent the true number of passes (i.e. the over-and-under passes) and the number of rows per pass, respectively.

3.1. Cross-flow heat exchanger with one pass and n rows

In this subsection the proposed methodology is validated and analyzed through comparison of the simulated results with ε–NTU analytical relations for one pass and n rows cross-flow heat exchanger. The six analytical relations considered are included in Table 1 [7–9]. For an unmixed/unmixed flow arrangement two relations were considered. One, Eq. (19), is the infinite series solution obtained by Mason and used in [8] and [9]. Another, Eq. (20), is extensively used in literature and is taken from [7]. An explanation of the origin of some terms of this equation can be found in [10].

We compare the maximum relative error between analytical (ε_t), Eqs. (15)–(18) (Table 1), and simulated (ε_s) effectiveness values, $G_{1,1}$, $G_{1,2}$, $G_{1,3}$, and $G_{1,4}$, respectively. This comparison is performed considering the available analytical expressions up to four rows. A maximum relative error is obtained from 1111 effectiveness values calculated in the following intervals $0 \leqslant C_i^* \leqslant 1$

Table 1
ε–NTU relationships for one-pass cross-flow configurations with one or more rows (Eqs. (15)–(18) from [7,8]; Eq. (19) from [8,9]; Eq. (20) from [7])

N_r	Side of C_{min}	Relation	Equation
1	A	$\varepsilon_A = 1 - e^{-\left(1-e^{\mathrm{NTU}_A \cdot C_A^*}\right)/C_A^*}$	(15)
2	A	$\varepsilon_A = 1 - e^{-2K/C_A^*}\left(1+\dfrac{K^2}{C_A^*}\right), \quad K = 1 - e^{-\mathrm{NTU}_A \cdot C_A^*/2}$	(16)
3	A	$\varepsilon_A = 1 - e^{-3K/C_A^*}\left(1+\dfrac{K^2(3-K)}{C_A^*}+\dfrac{3K^4}{2(C_A^*)^2}\right), \quad K = 1 - e^{-\mathrm{NTU}_A \cdot C_A^*/3}$	(17)
4	A	$\varepsilon_A = 1 - e^{-4K/C_A^*}\left(1+\dfrac{K^2(6-4K+K^2)}{C_A^*}+\dfrac{4K^4(2-K)}{(C_A^*)^2}+\dfrac{8K^6}{3(C_A^*)^3}\right),$ $K = 1 - e^{-\mathrm{NTU}_A \cdot C_A^*/4}$	(18)
∞	Both fluids unmixed	$\varepsilon = \dfrac{1}{C^*\mathrm{NTU}}\sum_{n=0}^{\infty}\left\{\left[1-e^{-\mathrm{NTU}}\sum_{m=0}^{n}\dfrac{(\mathrm{NTU})^m}{m!}\right]\left[1-e^{-C^*\mathrm{NTU}}\sum_{m=0}^{n}\dfrac{(C^*\mathrm{NTU})^m}{m!}\right]\right\}$	(19)
∞	Both fluids unmixed	$\varepsilon = 1 - e^{\left[\mathrm{NTU}^{0.22}\left(e^{-C^*\mathrm{NTU}^{0.78}}-1\right)/C^*\right]}$	(20)

Fluid A mixed, fluid B unmixed, $C_A^* = 1/C_B^*$, $\varepsilon_B = \varepsilon_A C_A^*$, $\mathrm{NTU}_B = \mathrm{NTU}_A C_A^*$, $C_A^* = C_A/C_B$.

Table 2
Comparison between model prediction and infinite series solution, Eq. (19)

N_r	Geometry	Average relative error (%)[a] and maximum relative error (%)			
		$C_{min} = C_{air}$		$C_{min} = C_t$	
5	$G_{1,5}$	0.63	2.88	0.45	2.89
6	$G_{1,6}$	0.44	2.10	0.32	2.10
7	$G_{1,7}$	0.33	1.56	0.24	1.56
8	$G_{1,8}$	0.25	1.22	0.18	1.22
9	$G_{1,9}$	0.20	0.97	0.14	0.97
10	$G_{1,10}$	0.16	0.79	0.12	0.79
20	$G_{1,20}$	0.04	0.20	0.03	0.20
50	$G_{1,50}$	0.006	0.033	0.005	0.033
100	$G_{1,100}$	0.0016	0.0082	0.0012	0.0082

[a] Average relative error $= \frac{1}{N}\sum_1^N \frac{|\varepsilon_s - \varepsilon_t|}{\varepsilon_t} 100$.

and $0 \leqslant \mathrm{NTU}_i \leqslant 10$ with 0.1 increment, respectively. Results shows that the maximum relative error is very small for all cases, i.e., relative error of the order of 10^{-6}%, indicating a perfect agreement between analytical and simulated values and the rigorousness of the present methodology. It should be emphasized that the simulation results obtained by the program are very accurate for any number of tube rows as we can see next.

Table 2 shows the convergence history of the simulation results to the infinite analytical solution, Eq. (19), for an unmixed–unmixed arrangement. Three main points can be emphasized from this comparison. First, it is observed that the maximum relative error decreases with the increase of the number of tube rows, being equal to 0.0082% for $N_r = 100$. This expected behavior shows the high accuracy of the developed methodology and indicates that if it is desired a smaller error a number of tube rows should be increased. This leads to the second main point of this comparison related to the unmixed fluid concept. From Table 2 it is seen that for a cross-flow heat exchanger have a completely unmixed–unmixed flow distribution it should have a higher enough number of tube rows to guarantee a small relative error in effectiveness.

The third main point is related to the fact that the analytical solution is valid rigorously only for an infinite number of tube rows and there are not easily available analytical formulae for more than four rows. So, the developed methodology permits to obtain very accurate data for geometry configurations for what the effectiveness values information is scarce or approximate formulae are used (see Eq. (20)). To make this point clearer the heat exchanger with one tube row is analyzed. Taking the point $C^* = 0.5$ and NTU = 5 it can be shown that an error of the order of 0.1% in the effectiveness provokes an error on the NTU of the order of 4.0% using then NTU-ε analytical relation. It points to the fact that even a small relative error on effectiveness can lead to a great error on NTU determination. Thus, caution should be taken when it is computed NTU from the effectiveness–NTU relations. One application where this is very important is the effectiveness–NTU reduction method, commonly used for experimental determination of the airside convective heat transfer coefficient. In Table 2 it is seen that even for 10 tube rows the average relative error on effectiveness is of the order of 0.1%. When the number of rows is augmented the error decreases as expected.

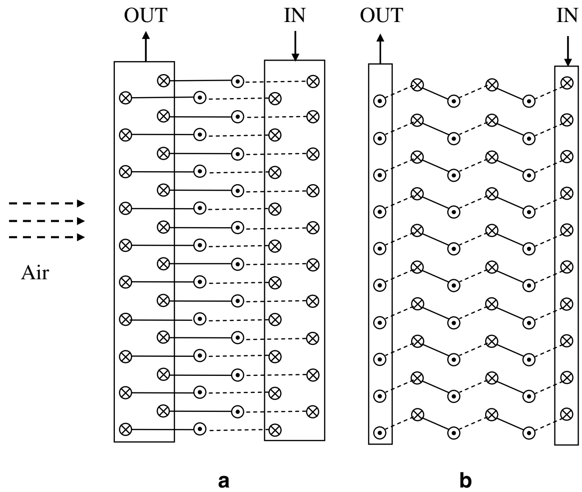

Fig. 3. Geometries and flow arrangement configurations for cases taken from [6]: (a) case 4 and (b) case 7 (× and ● signs indicates that fluid flows into or out of the paper, respectively).

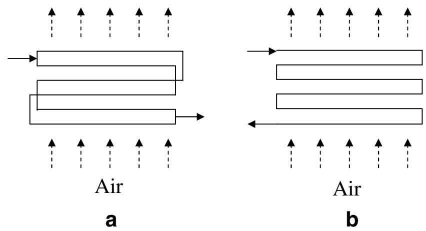

Fig. 4. Equivalent two dimensional geometries as proposed in [6] and simulated by the computational program: (a) case 4 and (b) case 7.

As it is difficult to derive analytical or polynomial relations for $N_r = 5$ to ∞, the approximate empirical correlation (Eq. (20)) is extensively used in industry and research laboratories. According to DiGiovanni and Webb [10] this correlation yields to unphysical results for NTU < 1, leading to a maximum error of 3.7% when compared with the numerical solution for an unmixed–unmixed case. Then, the proposed methodology supply more accurate results in these cases and can be used when an analytical relation is not available.

Table 3
Thermal effectiveness P values for cases 4 and 7 (Figs. 3 and 4) considering four, six and eight rows, with 10 tubes each

R	NTU	Thermal effectiveness P						
		Case 4			Case 7			Counter flow
		Four rows	Six rows	Eight rows	Four rows	Six rows	Eight rows	
0.2	0.2	0.1782	0.1782	0.1782	0.1782	0.1782	0.1782	0.1782
0.2	0.5	0.3802	0.3805	0.3806	0.3806	0.3806	0.3807	0.3807
0.2	1.0	0.6026	0.6039	0.6044	0.6043	0.6047	0.6049	0.6050
0.2	2.0	0.8245	0.8285	0.8299	0.8293	0.8306	0.8311	0.8317
0.2	5.0	0.9762	0.9814	0.9831	0.9819	0.9839	0.9845	0.9853
0.2	10.0	0.9968	0.9988	0.9993	0.9987	0.9994	0.9996	0.9997
0.5	0.2	0.1737	0.1737	0.1738	0.1738	0.1738	0.1738	0.1738
0.5	0.5	0.3610	0.3617	0.3620	0.3619	0.3621	0.3622	0.3623
0.5	1.0	0.5593	0.5623	0.5633	0.5631	0.5640	0.5643	0.5647
0.5	2.0	0.7577	0.7669	0.7702	0.7689	0.7720	0.7732	0.7746
0.5	5.0	0.9222	0.9404	0.9474	0.9421	0.9506	0.9535	0.9572
0.5	10.0	0.9660	0.9835	0.9896	0.9817	0.9913	0.9940	0.9966
1.0	0.2	0.1664	0.1666	0.1666	0.1666	0.1666	0.1666	0.1667
1.0	0.5	0.3312	0.3324	0.3328	0.3328	0.3331	0.3332	0.3333
1.0	1.0	0.4916	0.4962	0.4978	0.4974	0.4988	0.4994	0.5000
1.0	2.0	0.6422	0.6549	0.6597	0.6578	0.6626	0.6644	0.6667
1.0	5.0	0.7729	0.7996	0.8121	0.8020	0.8183	0.8246	0.8333
1.0	10.0	0.8178	0.8532	0.8713	0.8483	0.8772	0.8898	0.9091
1.5	0.2	0.1141	0.1142	0.1142	0.1142	0.1142	0.1142	0.1142
1.5	0.5	0.2338	0.2344	0.2346	0.2346	0.2348	0.2348	0.2349
1.5	1.0	0.3572	0.3597	0.3606	0.3605	0.3612	0.3615	0.3618
1.5	2.0	0.4793	0.4866	0.4893	0.4885	0.4911	0.4920	0.4932
1.5	5.0	0.5879	0.6021	0.6085	0.6049	0.6120	0.6148	0.6186
1.5	10.0	0.6250	0.6404	0.6473	0.6402	0.6501	0.6537	0.6586
3.0	0.2	0.0587	0.0587	0.0587	0.0587	0.0587	0.0587	0.0588
3.0	0.5	0.1238	0.1240	0.1241	0.1241	0.1241	0.1241	0.1241
3.0	1.0	0.1943	0.1951	0.1953	0.1953	0.1955	0.1956	0.1957
3.0	2.0	0.2650	0.2672	0.2680	0.2678	0.2685	0.2688	0.2691
3.0	5.0	0.3198	0.3225	0.3236	0.3231	0.3243	0.3247	0.3253
3.0	10.0	0.3310	0.3322	0.3326	0.3323	0.3327	0.3329	0.3330
7.0	0.2	0.0256	0.0256	0.0256	0.0256	0.0256	0.0256	0.0256
7.0	0.5	0.0548	0.0549	0.0549	0.0549	0.0549	0.0549	0.0549
7.0	1.0	0.0873	0.0874	0.0875	0.0875	0.0875	0.0875	0.0875
7.0	2.0	0.1194	0.1199	0.1200	0.1200	0.1201	0.1202	0.1202
7.0	5.0	0.1405	0.1408	0.1410	0.1409	0.1410	0.1411	0.1412
7.0	10.0	0.1428	0.1428	0.1428	0.1428	0.1428	0.1428	0.1428

3.2. *Analysis of some cross-flow heat exchanger's complex configurations*

A good predictive capacity of the developed methodology is presented in this subsection, where comparisons between approximate solutions and simulation results are showed for multipass counter cross-flow heat exchangers. There are considered two cases studied by [6]. The authors examine a very complicated heat exchanger flow arrangement, relating them to standard cross-flow configurations using the Domingos' [11] rules. These standard configurations were described by exact or approximate solutions using the recursive algorithms presented in [12].

More specific, they consider seven possible flow arrangements for a cross-flow heat exchanger of 60 tubes, arranged in six rows of 10 tubes each. Values for thermal effectiveness were obtained and a comparative analysis was performed. In this subsection are considered the cases 4 and 7 by [6] to illustrate the present methodology.

In Fig. 3 are shown schematically the geometry and flow arrangement configuration of the above two cases taken from [6]. For these two configurations, the authors obtained the relations (21) (case 4) and (22) (case 7) for thermal effectiveness of the out of tube fluid, denoted as P

$$P(R,\mathrm{NTU}) = P^{\mathrm{c,so}}_{3,2}(R,\mathrm{NTU}) \tag{21}$$

$$P(R,\mathrm{NTU}) = P^{\mathrm{c}}_{6,1}(R,\mathrm{NTU}) \tag{22}$$

In these relations $P^{\mathrm{c,so}}_{3,2}$ and $P^{\mathrm{c}}_{6,1}$ represent the effectiveness for a three true pass, with two-row per pass connected in the same order and for a six true pass, with one row per pass cross-counter flow exchangers, respectively. For calculation of these two effectiveness data, the recursive algorithm presented in [12] was used by [6]. The values obtained from Eqs. (21) and (22) are found in Table 1 of [6] and will be considered for comparison with the simulation results for the effectiveness P obtained in this work.

For this purpose two calculations are performed for each analyzed case. Taking as an example the case 4, the geometry shown in Fig. 3(a) is simulated. Then, the equivalent geometry (Fig. 4(a)), proposed by [6], corresponding to a standard flow arrangement representing the effectiveness $P_{3,2}^{c,so}$ is also simulated. The same procedure is done for the case 7 (Figs. 3 and 4(b)). Thus, the proposed methodology is tested twice showing its flexibility and the possibility of proving of the effectiveness calculation methods.

Table 3 shows effectiveness P data for R equal to 0.2, 0.5, 1.0, 1.5, 3.0 and 7.0 for the geometries showed in Fig. 3 and NTU varying from 0.2 to 10. Data for similar geometries to those of cases 4 and 7 (see Fig. 3) but considering four and eight rows with 10 tubes each are also presented. The results for the geometries represented in Fig. 4 are not showed because they are exactly equal to those of Fig. 3, in all cases. The simulated effectiveness values for the considered geometries (Figs. 3 and 4) matched exactly those presented in [6] for $R \leqslant 1$, showing the rigorousness of the present method. For $R > 1$, it was verified that results presented in [6] are less accurate, at least for the cases 4 and 7, including the counter flow arrangement. In this range of R values, the data presented in Table 3 are very accurate and new. As expected, the effectiveness increases with the number of tube rows augmentation, tending to the counter flow configuration values, also showed in Table 3 for comparison purpose. Similarly to [6], although the number of tabulated values in Table 3 is too high, they are presented because could be used for interpolation and for applications that may require a wider range of NTU and R values. Moreover, the results shown in Table 3 are new (for $R > 1$) and very accurate for all range of R including values for four and eight rows not shown in the paper of Shah and Pignotti [6].

From this analysis it is concluded that the developed methodology allows the study of any configuration directly, without the necessity of application of the available literature procedures, which are very strong, but can be difficult to apply. In the two analyzed cases, although Shah and Pignotti present a new method of computation of the effectiveness in analytical form, its method needs a recursive algorithm developed by Pignotti and Cordero [12] to perform all the computations for the standard configurations. This recursive algorithm should be resolved in a computer as the present procedure.

4. Conclusions

This paper presents a new methodology for cross-flow heat exchanger thermal performance computation. For this purpose a computational program *HETE* (*Heat Exchanger Thermal Efficiency*) is implemented. The proposed methodology is validated through comparison with well-established analytical and approximate theoretical results from research works, obtaining very small errors. New effectiveness data are obtained for some complex flow arrangements. The following final remarks can be stressed in relation to the proposed methodology:

- It is based on physical concepts and it is characterized by the division of the heat exchanger in a number of small and simple one-pass mixed–unmixed cross-flow heat exchangers.
- It has a simpler form (Section 2), and therefore can be easily used by other researchers in the design, rating and analysis of several cross-flow heat exchangers configurations.
- It is very accurate and therefore suitable for predicting the performance of several cross-flow heat exchangers, including heat exchangers with new and complex flow arrangements where analytical or approximate solutions are not disposable.
- It permits to obtain data for cross-flow heat exchangers configurations using the ε–NTU, LMTD, *P*–NTU and other methods, including the obtainment of polynomial curves, graphics and correlations.

Summary, due the prediction capability, the developed methodology here described represents a useful research tool for theoretical and experimental studies in heat exchangers performance research. It therefore contributes to the improvement of the energy resources use and management.

Acknowledgements

The authors would like to acknowledge Professor José Maria Saiz Jabardo by his contribution and guidance to this work. The authors acknowledge the support obtained from FAPESP (Fundação de Amparo a Pesquisa do Estado de São Paulo) specifically through a doctor and postdoctoral scholarships for the second author (processes 98/13812-1 and 02/12038-8).

References

[1] Th. Bes, Thermal performance of codirected cross-flow heat exchangers, Heat Mass Transfer 31 (1996) 215–222.
[2] D.P. Sekulic, R.K. Shah, A. Pignotti, A review of solution methods for determining effectiveness–NTU relationships

for heat exchangers with complex flow arrangements, Appl. Mech. Rev. 52 (3) (1999) 97–117.

[3] A. Pignotti, R.K Shah, Effectiveness–number of transfer units relationships for heat exchanger complex flow arrangements, Int. J. Heat Mass Transfer 35 (1992) 1275–1291.

[4] W.M. Kays, A.L. London, Compact Heat Exchangers, third ed., McGraw Hill, New York, 1998.

[5] R.K. Shah, D.P. Sekulic, Heat exchangers, in: W.M. Roshenow, J.P. Hartnett, Y.I. Cho (Eds.), Handbook of Heat Transfer, third ed., McGraw Hill, NewYork, 1998 (Chapter 17).

[6] R.K. Shah, A. Pignotti, Thermal analysis of complex cross-flow exchangers in terms of standard configurations, ASME J. Heat Transfer 115 (1993) 353–359.

[7] ESDU 86018, Effectiveness–NTU relations for the design and performance evaluation of two-stream heat exchangers, Engineering Science Data Unit 86018 with amendment, London ESDU International plc, 1991, pp. 92–107.

[8] R.A. Stevens, J. Fernandez, J.R. Woolf, Mean-temperature difference in one, two, and three-pass crossflow heat exchangers, Trans. ASME 79 (1957) 287–297.

[9] B.S. Baclic, P.J. Heggs, On the search for new solutions of the single-pass crossflow heat exchanger problem, Int. J. Heat Mass Transfer 28 (10) (1985) 1965–1975.

[10] M.A. DiGiovanni, R.L. Webb, Uncertainty in effectiveness–NTU calculations for crossflow heat exchangers, Heat Transfer Eng. 10 (3) (1989) 61–70.

[11] J.D. Domingos, Analysis of complex assemblies of heat exchangers, Int. J. Heat Mass Transfer 12 (1969) 537–548.

[12] A. Pignotti, G. Cordero, Mean temperature difference in multipass crossflow, ASME J. Heat Transfer 105 (1983) 584–591.